

A colorimetric chemosensor for both fluoride and transition metal ions based on dipyrrolyl derivative

Tamal Ghosh, Bhaskar G. Maiya† and Anunay Samanta*

Received 22nd July 2005, Accepted 23rd December 2005

First published as an Advance Article on the web 13th January 2006

DOI: 10.1039/b510469f

The synthesis, characterization and ion binding studies of 2,3-di(1*H*-2-pyrrolyl)pyrido[2,3-*b*]pyrazine (**1**) have been described. **1**, which has been targeted with a view to sensing both F⁻ and transition metal ions, exhibits binding-induced color changes from yellowish green to red/brown observable by the naked eye. The binding site for the metal ion in the system has been unambiguously established by single-crystal X-ray diffraction study of a Ni(II) complex of **1**. While the estimated value of the binding constant of **1** with F⁻ is $4.9 \times 10^3 \text{ M}^{-1}$, the binding constants for the cations are found to be two orders higher in magnitude in acetonitrile. Even though **1** possesses two separate binding sites for F⁻ and metal ions, it is shown that the presence of the cation influences the binding of the anion and *vice versa*. The binding constant values of an ion in the presence of oppositely charged species are measured to be significantly lower.

Introduction

Development of chemosensors capable of recognizing and sensing cations and anions is one of the most challenging fields, not only from the viewpoint of organic and supramolecular chemistry but also from its potential clinical applications.¹⁻³ Chemosensors consist of signaling (chromophore/fluorophore) and guest binding (receptor) moieties, either separated by a spacer or integrated into one unit. Generally, N or O donor centers act as binding sites for cations¹ and pyrrole, -OH, -NH₂, -CONH, -NH₃⁺ *etc.* (capable of forming hydrogen bonds) or boron, silicon (capable of forming Lewis adducts) centers act as binding sites for anions.² Simultaneous sensing of both types of charged analytes has been achieved by integrating cationic and anionic guest binding sites in a single molecule, where the cation binding site binds with a transition (Ni²⁺, Cu²⁺, Ag⁺, Cd²⁺) or alkali (Li⁺, Na⁺, K⁺) or alkaline earth metal ion (Mg²⁺, Ca²⁺).^{4,5}

During recent years, there is an upsurge in the field of colorimetric sensing of alkali, alkaline-earth and transition metal ions by organic molecules.⁶ Among the cations, special attention is devoted to develop chemosensors for transition metal ions: usually they symbolize an environmental concern when present in uncontrolled amount but at the same time some of them such as iron, cobalt, copper, zinc are present as essential elements in biological systems. On the other hand, the halides, especially fluoride ion is of major interest among the anions due to its detrimental role (fluoresis and other diseases).⁷ The recently reported pyrrole-based sensors namely, calix[4]pyrrole,⁸ dipyrrolylquinoxaline (DPQ)⁹⁻¹⁵ and dipyrrolylpyrazine (DPP)¹⁶⁻¹⁸ families of compounds have been used for anion sensing by exploiting the hydrogen bond forming ability of pyrrole NH with anions, with subsequent change in color or fluorescence or redox potential. The last two

types of sensors have the dual advantage of possessing a built-in chromophore and being readily accessible in two steps from commercially available materials.

We have recently embarked upon designing systems that can sense both anions and metal ions. To begin with, we concentrated on systems that can sense both transition metal ions and fluoride ion. In order to accomplish this goal, we have exploited the fluoride ion signaling potential of the DPP derivatives and transition metal ion binding ability of the pyridine moiety. Amalgamating these approaches we have developed **1**, wherein a pyridine ring has been fused with the pyrazine frame. We demonstrate here unequivocally that it is indeed the nitrogen atom of the pyridine moiety that binds the transition metal ions. It is shown that this new DPP derivative binds the metal ions much more strongly compared to the previously reported DPP derivative which lacks the additional fused pyridine ring.¹⁶⁻¹⁸ The sensing of F⁻ and metal ions (Co²⁺, Ni²⁺, Cu²⁺, Zn²⁺ and Cd²⁺) by **1** in acetonitrile is observable by change in color from yellowish green to red in the case of the former and to brown or light brown in the later cases. The binding constants of the cations are found to be two orders of magnitude higher than that of F⁻.

Experimental

Syntheses

The starting material 1,2-di(1*H*-2-pyrrolyl)-1,2-ethanedione (**2**)^{9,19} used for synthesis of **1** and the model compound pyrido[2,3-*b*]pyrazine (**3**)²⁰ were prepared by procedures published elsewhere. The new sensor investigated in this study and its Ni(II) complex were synthesized as detailed below.

2,3-Di(1*H*-2-pyrrolyl)pyrido[2,3-*b*]pyrazine (1). Diketone **2** (190 mg, 1.0 mmol) was dissolved in toluene (40 mL), and a catalytic amount of BF₃·Et₂O was added to it. A hot solution of 2,3-diaminopyridine (120 mg, 1.1 mmol) in toluene (30 mL) was

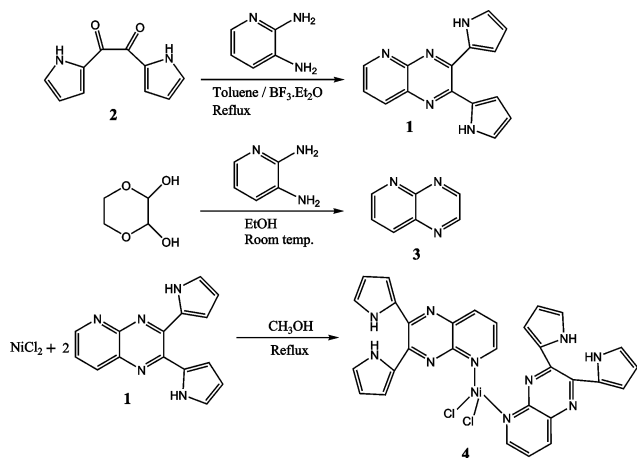
School of Chemistry, University of Hyderabad, Hyderabad, 500 046, India.
E-mail: assc@uohyd.ernet.in; Fax: (+91) 40-2301-2460

† Deceased.

added with stirring. The resulting mixture was heated at reflux under nitrogen atmosphere for 8 h. Then, toluene was distilled off under vacuum and the residue was taken up in a mixture of CH_2Cl_2 (50 mL) and water (50 mL). The organic layer was separated off and the aqueous layer was extracted with CH_2Cl_2 (3×30 mL). The organic layers were combined and dried over anhydrous sodium sulfate, filtered and evaporated to dryness. Column chromatography over neutral alumina (eluent: CH_2Cl_2 –MeOH, 99 : 1, v/v) afforded **1** (160 mg, 61%) as a yellow solid. Anal. Calc. for $\text{C}_{15}\text{H}_{11}\text{N}_5$: C, 68.96; H, 4.21; N, 26.83. Found: C, 69.19; H, 4.28; N, 26.54%. ^1H NMR (400 MHz, CDCl_3 , TMS) δ /ppm: 6.25–6.28 (1H, m), 6.30–6.33 (1H, m), 7.04–7.06 (2H, m), 7.10–7.12 (1H, m), 7.17–7.19 (1H, m), 7.50 (1H, dd, $J = 4.0$ Hz, 8.0 Hz), 8.21 (1H, dd, $J = 2.0$ Hz, 8.0 Hz), 8.91 (1H, dd, $J = 2.0$ Hz, 4.0 Hz), 9.60 (1H, br s), 10.04 (1H, br s). ^{13}C NMR (50 MHz, CDCl_3 – CD_3OD , 3 : 1, v/v, TMS) δ /ppm: 159.5, 152.8, 150.0, 148.7, 147.2, 138.7, 135.8, 129.7, 125.1, 124.8, 123.2, 116.5, 114.9, 111.2, 110.9; mp 155 ± 1 °C. FAB-MS: m/z 262 ($\text{M} + \text{H}^+$); UV-Vis (CH_3CN) λ_{max} /nm ($\epsilon/\text{M}^{-1} \text{cm}^{-1}$): 204 (25190), 263 (18220), 312 (7080), 350 (7810), 421 (12360).

1,2-Di(1H-2-pyrrolyl)-1,2-ethanedione (2). This was synthesized as per the reported procedure published elsewhere.^{9,19} Anal. Calc. for $\text{C}_{10}\text{H}_8\text{N}_2\text{O}_2$: C, 63.83; H, 4.25; N, 14.89. Found: C, 64.05; H, 4.20; N, 14.63%. ^1H NMR (200 MHz, $(\text{CD}_3)_2\text{SO}$, TMS) δ /ppm: 6.25 (2H, m), 6.91 (2H, m), 7.34 (2H, m), 12.22 (2H, br s). UV-Vis (CH_2Cl_2) λ_{max} /nm ($\epsilon/\text{M}^{-1} \text{cm}^{-1}$): 340 (15730).

Pyrido[2,3-*b*]pyrazine (3). This was synthesized as per the reported procedure shown in Scheme 1.²⁰ Anal. Calc. for $\text{C}_7\text{H}_5\text{N}_3$: C, 64.12; H, 3.82; N, 32.06. Found: C, 64.25; H, 3.96; N, 31.90%. ^1H NMR (400 MHz, CDCl_3 , TMS) δ /ppm: 7.77 (1H, d, $J = 3.6$ Hz, 8.8 Hz), 8.51 (1H, dd, $J = 2.0$ Hz, 8.8 Hz), 8.70 (1H, d, $J = 1.6$ Hz), 9.10 (1H, d, $J = 1.6$ Hz), 9.22 (1H, dd, $J = 2.0$ Hz, 4.0 Hz). ^{13}C NMR (50 MHz, CDCl_3 , TMS) δ /ppm: 154.3, 151.4, 147.8, 146.1, 138.6, 138.2, 125.4; mp 146 ± 1 °C (lit.,²⁰ 146–147 °C). LC-MS: m/z 131 (M^+); UV-Vis (CH_3CN) λ_{max} /nm ($\epsilon/\text{M}^{-1} \text{cm}^{-1}$): 255 (1890), 301 (6760), 308 (7010), 314 (8970), 354 (220).



Scheme 1 Synthesis of **1**, **3** and **4**.

Dichlorobis(2,3-di(1H-2-pyrrolyl)pyrido[2,3-*b*]pyrazine)nickel(II) (4). 38 mg (0.14 mmol) of **1** was dissolved in methanol and 17 mg (0.07 mmol) of NiCl_2 (in methanol) was added. The solution

was refluxed for 3 h and the solvent was evaporated to dryness. The red solid was recrystallised from acetonitrile. Anal. Calc. for $\text{C}_{30}\text{H}_{22}\text{N}_{10}\text{NiCl}_2$: C, 55.19; H, 3.37; N, 21.46. Found: C, 55.34; H, 3.42; N, 21.28%.

Instrumentation and methods

Hydrated perchlorate salts of the metals were used for cation titrations. All anions, in the form of tetrabutylammonium salts, were stored in a desiccator under vacuum containing self-indicating silica and used for titration without any further purification. Pyrrole (Ranbaxy Acros, Belgium) was dried over CaH_2 (Ranbaxy, Mumbai, India) and distilled under reduced pressure. All solvents used in the spectroscopic studies were purchased from Ranbaxy (Mumbai, India) and were distilled as per requirement by the published procedures.²¹ CDCl_3 , $(\text{CD}_3)_2\text{SO}$ and CD_3OD were purchased from Merck (Germany).

Care was taken to avoid the entry of direct, ambient light into the samples in all the spectroscopic experiments described below. Unless otherwise specified, all the experiments were carried out at 298 ± 1 K.

The single crystals of **1** and **4** for X-ray diffraction studies were grown by slow evaporation of acetonitrile solutions of the compounds. Single-crystal X-ray data was collected on a Bruker-Nonius SMART APEX CCD single-crystal diffractometer at 298 K, equipped with a graphite monochromator and a Mo- $\text{K}\alpha$ fine-focus sealed tube ($\lambda = 0.71073$ Å) operated at 2.0 kW. The SMART software was used for data acquisition. The detector frames were integrated by use of the program SAINT-Plus and the intensities corrected for absorption by Gaussian integration using the program SADABS. The structure solution was carried out using direct methods. Full-matrix least-squares refinement on F^2 (including all data) was performed using the program SHELXTL.²² The PLATON package was used for molecular graphics.²² All non-hydrogen atoms were refined with anisotropic thermal parameters. Hydrogen atoms attached to pyrrole nitrogens were located from difference Fourier maps. All other hydrogen atoms were fixed in their ideal geometric positions.

CCDC reference numbers 279117 and 279118.

For crystallographic data in CIF or other electronic format see DOI: 10.1039/b510469f

The ^1H and ^{13}C NMR spectra were recorded on a Bruker NR-200 AF-FT or Bruker AVANCE 400 NMR spectrometer at ambient temperature using tetramethylsilane (TMS) as an internal standard. UV-Visible spectra were recorded on a Shimadzu UV-3101 PC spectrophotometer. A matched pair of quartz cuvettes (path length = 1 cm) were employed for this purpose. Steady-state fluorescence spectra were recorded in a four-walled, all-transparent, quartz cell (path length = 1 cm) using a FluoroMax-3 (Jobin Yvon-Spex) spectrofluorimeter for solutions having low optical densities at the wavelengths of excitation. The fluorescence quantum yield (ϕ_f) was estimated by integrating the fluorescence band and by using 1,6-diphenyl-1,3,5-hexatriene ($\phi_f = 0.80$ in cyclohexane)²³ as the standard.

Absorption titration studies

The binding studies of sensor **1** against different cations and anions were carried out in CH_3CN . Typically, a solution of 6.5 μM of **1**

was taken in the cuvette and titrated with increasing volume of concentrated solution of a given cation or anion. The binding constant (K) between **1** and cation/anion was evaluated from the change in absorbance at 490 nm by the following method.^{24,25}

The binding constant (K) for 1 : 1 complexation can be represented as

$$K = \frac{[C]}{([F]_0 - [C])([M]_0 - [C])} \quad (1)$$

where, $[C]$ represents the equilibrium concentration of the complex and $[F]_0$ and $[M]_0$ represent the initial concentration of the sensor and metal ion/anion, respectively.

By substituting the term $\Delta A/\Delta \epsilon$ for $[C]$ (for a path length of 1 cm) the following equation can be derived,

$$\frac{[F]_0[M]_0}{\Delta A} = \left([F]_0 + [M]_0 - \frac{\Delta A}{\Delta \epsilon} \right) \frac{1}{\Delta \epsilon} + \frac{1}{K\Delta \epsilon} \quad (2)$$

where, ΔA is the change in absorbance due to the addition of cation/anion, $[F]_0$ is the initial concentration of **1**, $[M]_0$ is the concentration of cation/anion, $\Delta \epsilon$ is the difference between the molar extinction coefficient of the complex and **1** and K is the binding constant.

A plot of $[F]_0[M]_0/\Delta A$ vs. $([F]_0 + [M]_0 - (\Delta A/\Delta \epsilon))$ would yield a straight line with slope $1/\Delta \epsilon$ and intercept $1/K\Delta \epsilon$. However, knowledge of the unknown quantity $\Delta \epsilon$ is needed to make this plot.

Consequently, a tentative value of $\Delta \epsilon$ is determined by using data from two solutions and solving eqn (2) simultaneously for $\Delta \epsilon$ and K . Using this value of $\Delta \epsilon$ a plot is made employing data from a series of solutions, and a new value of $\Delta \epsilon$ is determined along with a new value of K . This procedure is repeated until a consistent set of values for both $\Delta \epsilon$ and K have been obtained from two successive plots.

For anions, the binding constant was also evaluated by the change in absorbance at 490 nm with anion concentration using the following non-linear equation.²⁵

$$\frac{\Delta A}{b} = \frac{Q_1 K \Delta \epsilon [L]}{1 + K[L]} \quad (3)$$

where, ΔA refers to the change in absorbance from initial value at the required wavelength, b is cuvette path length (in cm), Q_1 is total concentration of sensors, K is the binding constant between **1** and anion, $\Delta \epsilon$ is the difference between the molar extinction coefficient of free and bound sensor and $[L]$ is the concentration of titrated anion. The K values obtained by the two methods agreed reasonably well (within $\pm 10\%$).

Results and discussion

The scheme leading to the synthesis of **1**, **3** and **4** is illustrated in Scheme 1. Reaction between 1,2-di(1*H*-2-pyrrolyl)-1,2-ethanedione (**2**) and 2,3-diaminopyridine produced sensor **1** in $\sim 60\%$ yield. Sensor **1** can be considered structurally as a DPP derivative, well known for its potential as an F^- sensor, having an additional pyridine ring fused with the pyrazine ring as part of its extended π framework. The justification behind the fusion of the pyridine ring is to make **1** work as a cation sensor as well. This is because pyridine can act as a cation binding centre in a sensor molecule.²⁶ In fact, a stronger metal binding property of

1 compared to a previously reported DPP derivative^{16–18} supports our above justification (*vide* Cation sensing section).

X-Ray structures of **1** and **4**

In order to determine whether one of the pyrazine nitrogen atoms or the pyridine nitrogen atom or both are involved in interaction with the metal ions, the Ni(II) complex of **1**, *i.e.* **4** was synthesized and its structure obtained by X-ray diffraction analysis.

The solid-state structures of **1** and **4** are shown as an ORTEP diagram in Fig. 1 and the crystallographic data are shown in Table 1. There are major differences in the spatial orientation of the two pyrrole rings with respect to the pyridopyrazine plane. In the case of **1**, both the pyrrole rings are directed such that the pyrrole NH are on the same side of the pyrazine nitrogen atoms, the dihedral angles between pyrrole rings and pyridopyrazine plane being 23.2 and 36.1°. The picture is quite different in the case of **4**. Ni(II) is coordinated with the pyridine nitrogens of two molecules of **1** and two Cl^- , having a distorted tetrahedral geometry with the pyridine N–Ni–N bond angle 96.88° and Cl–Ni–Cl bond angle 99.75°. The two pyrrole NH bonds point to each other and both are in different planes from the fused pyridopyrazine ring plane. Here, all the dihedral angles between the pyrrole rings and pyridopyrazine ring of two ligands are different: 18.4 and

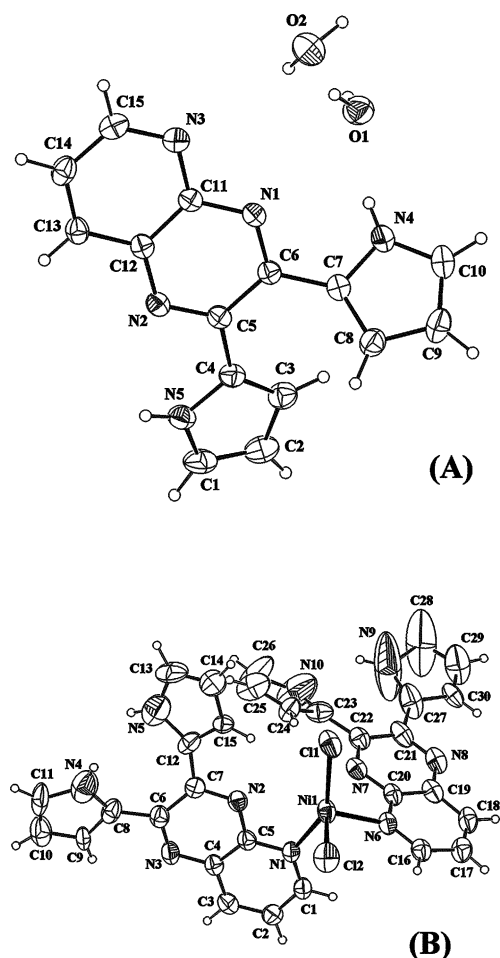


Fig. 1 X-Ray structures of (A) **1** and (B) **4**, with all heavy atoms labeled. The thermal ellipsoids were scaled to the 30% probability level.

Table 1 Crystallographic data for **1** and **4**

Ligand/Complex	1	4
Chemical formula	C ₁₅ H ₁₁ N ₅ ·2H ₂ O	NiC ₃₀ H ₂₂ Cl ₂ N ₁₀
Formula weight	297.32	652.19
Crystal system	Triclinic	Triclinic
Space group	<i>P</i> $\bar{1}$	<i>P</i> $\bar{1}$
<i>a</i> /Å	6.7615(6)	6.9445(4)
<i>b</i> /Å	9.3751(9)	12.8462(8)
<i>c</i> /Å	12.2200(11)	17.3296(11)
<i>a</i> /°	83.376(2)	110.3790(10)
<i>β</i> /°	89.496(2)	90.8100(10)
<i>γ</i> /°	75.250(2)	94.5210(10)
<i>V</i> /Å ³	743.92(12)	1443.28(15)
<i>Z</i>	2	2
<i>μ</i> /mm ⁻¹	0.093	0.898
<i>T</i> /K	298	298
Reflections collected	8661	13866
Unique reflections	3453	5058
Reflections [<i>I</i> ≥ 2σ(<i>I</i>)]	2678	3143
Parameters	219	388
<i>R</i> ₁ , <i>wR</i> ₂ [<i>I</i> ≥ 2σ(<i>I</i>)]	0.0651, 0.1874	0.0724, 0.1991
<i>R</i> ₁ , <i>wR</i> ₂ (all data)	0.0792, 0.2003	0.1103, 0.2241
Goodness-of-fit on <i>F</i> ²	1.059	1.040
Largest peak and hole/e Å ⁻³	1.034, -0.304	0.566, -0.532

20.6° in one ligand and 10.7 and 25.0° in the other. There are two molecules of **4** in unit cell but no intermolecular hydrogen bonding is observed like **1**. It is also important to note that only pyridine nitrogen is bonded with Ni(II), not the pyrazine nitrogen atoms. This observation is consistent with the recent finding of Manson, who has shown that the pyridine nitrogen atom of **3** is involved in coordination with Cu²⁺.²⁷

Spectral characterization

The UV-visible spectra of **1** and **3** in CH₃CN are depicted in Fig. 2. It can be seen that the spectrum of **1** appears as somewhat structured but it lacks the fine structure of the spectrum of **3**. Further, the lowest energy absorption band of **1** appears at a much longer wavelength relative to that of **3**. These observations are consistent with an extended π -conjugation and N–H···N interaction between the pyrrolic and pyrazinic rings in **1**.

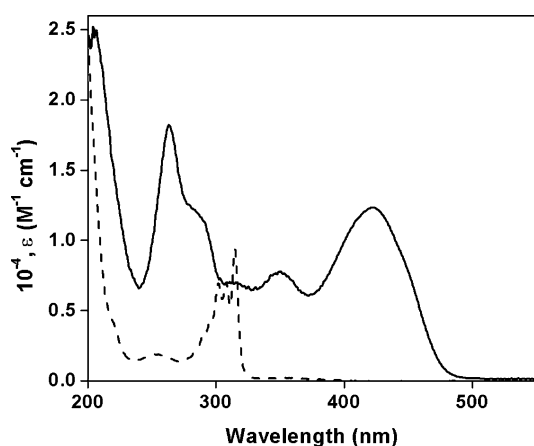


Fig. 2 Comparison of the absorption spectra of **1** (—) and **3** (---) in CH₃CN.

The influence of solvent on the absorption, fluorescence and fluorescence excitation spectra of **1** has been investigated in detail with a view to understanding the origin of the lowest energy transition in the absorption and fluorescence spectra. The fluorescence excitation spectrum of the system in any given solvent is found identical with the absorption spectrum in the same solvent. Fig. 3 shows the fluorescence and fluorescence excitation spectra of the systems. The most noticeable feature of these spectra is the loss of structure in polar media. That the band positions are not so sensitive to the polarity of the medium in the aprotic medium suggest that the charge transfer contribution in these transitions is minimal. Reasonably high molar extinction coefficient of the absorption band and fairly high fluorescence efficiency of **1** (see later) suggest that the lowest energy transition in absorption and fluorescence is π - π^* in nature. However, in protic media a blue shift of the absorption (or excitation) band suggests that an n - π^* state is in close proximity with the π - π^* state.²⁸ Since the blue shift is not observable in emission, it is evident that irrespective of the nature of the solvent, the emission always occurs from the π - π^* state, which is the lowest excited state in the system.

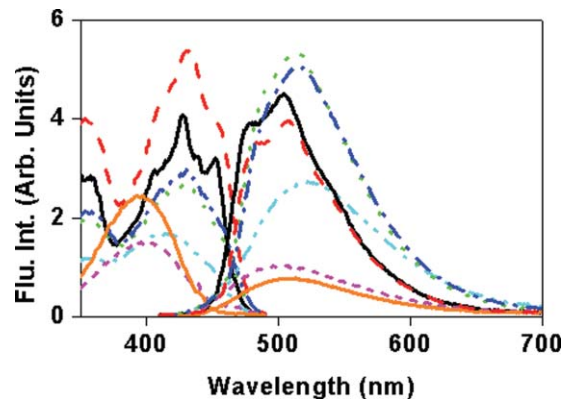


Fig. 3 Fluorescence excitation and fluorescence spectra of **1** in different solvents: cyclohexane (black, —), toluene (red, - -), 1,4-dioxane (green, ···), tetrahydrofuran (blue, - · -), acetonitrile (light blue, — · —), 2-propanol (purple, ---) and methanol (orange, —). Conditions for fluorescence excitation spectra of **1** in different solvents: $\lambda_{\text{em}} = 505$ nm, excitation and emission slit = 2 nm. Conditions for fluorescence spectra of **1** in different solvents: $\lambda_{\text{exc}} = 395$ nm, OD at 395 nm = 0.017, excitation and emission slit = 2 nm.

1 is found to be strongly fluorescent; the fluorescence quantum yield, ϕ_f value is estimated to be 0.29 in CH₃CN. We have also studied the fluorescence decay behavior of the system in tetrahydrofuran and acetonitrile. A single exponential fit to the decay profiles was found satisfactory from the χ^2 values and the residuals. The measured lifetimes are 2.5 ns in acetonitrile and 3.4 ns in tetrahydrofuran.

Fig. 4 illustrates the ¹H NMR spectrum of sensor **1**. The spectrum was analyzed (see Experimental section) based not only on the chemical shift and integrated intensity data of the various peaks appearing in the 1D spectra but also on the proton connectivity patterns observed in the corresponding ¹H-¹H COSY spectra. The four β -pyrrole protons resonate at four distinct signals as multiplets. While two of them (Hb and Hb') appear at upfield, other two (Hc and Hc') shift at downfield compared to Ha and Ha' in ¹H NMR spectrum. Also, one of the two pyrrolic NH protons

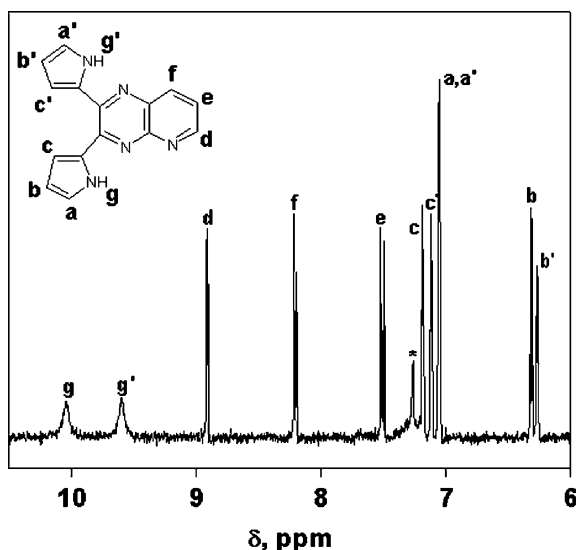


Fig. 4 ^1H NMR spectrum of **1** (CDCl_3 , TMS); * indicates the solvent signal for CDCl_3 .

appears 0.4 ppm downfield of the other. The pyrazine ring creates a non-equivalent magnetic environment for the pyrrole rings by virtue of intramolecular hydrogen bonding between pyrrole NH and pyrazine nitrogen, and the electron withdrawing conjugation effect of pyridine. However, the two α -pyrrole protons (Ha and Ha'), being unaffected by such an effect, appear together at 7.04–7.06 ppm.

Cation sensing

Fig. 5 shows typical changes in the absorption spectrum of **1** on addition of the metal salts in acetonitrile. The peak around 420 nm

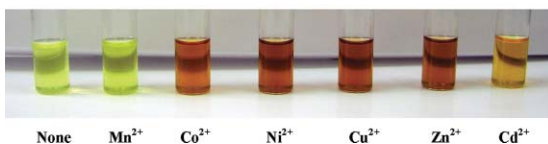
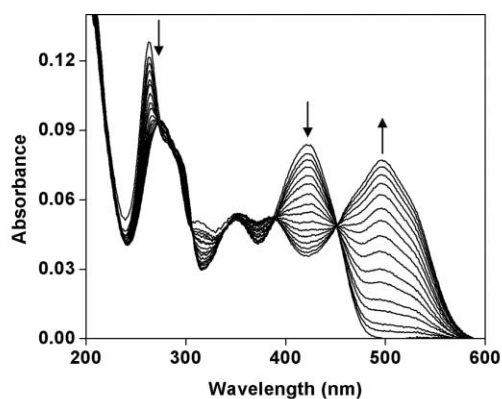


Fig. 5 Top: Absorption spectral changes observed for **1**, upon addition of Ni^{2+} ion in CH_3CN at 298 K. $[\text{1}] = 6.5 \times 10^{-6}$ M; $[\text{Ni}^{2+}] = (0, 0.33, 0.66, 1.16, 1.66, 2.32, 2.98, 3.80, 4.62, 5.60, 6.58, 7.71, 9.00, 10.44, 12.03, 13.93) \times 10^{-6}$ M. Bottom: Color changes observed for **1** in CH_3CN upon the addition of cations (as ClO_4^- salts). From left to right: none, Mn^{2+} , Co^{2+} , Ni^{2+} , Cu^{2+} , Zn^{2+} and Cd^{2+} .

Table 2 Cation^a and anion^b binding constants for **1** in CH_3CN determined by absorption titration method at 25 °C^c

Ion	$10^{-5} K/\text{M}^{-1}$
Mn^{2+}	ND ^d
Co^{2+}	3.2
Ni^{2+}	11.0
Cu^{2+}	15.0
Zn^{2+}	4.8
Cd^{2+}	0.68
F^-	0.049

^a Counter anion was perchlorate salts for all cases. ^b Counter cation was tetrabutylammonium salts. ^c All errors are $\pm 10\%$. ^d Change in UV-Visible spectra was not enough to calculate binding constant.

disappears and a new band appears at a much longer wavelength ($\lambda_{\text{max}} = 496$ nm). The presence of an isosbestic point implies that **1** and **1**· Ni^{2+} are in equilibrium in the course of titration. The spectral changes observed are similar for Co^{2+} , Cu^{2+} , Zn^{2+} and Cd^{2+} ions. The change in the absorbance at 490 nm has been used to calculate the binding constant, K , using eqn (2). That the sensor **1** binds the transition metal ions with varying degree of strength is evident from the binding constant values shown in Table 2. Ni^{2+} and Cu^{2+} bind more strongly ($K \sim 10^6 \text{ M}^{-1}$), compared to Co^{2+} and Zn^{2+} for which the K values are one order of magnitude less. The metal ion binding is associated with a color change from yellowish green to brown and is observable by naked eye. In the case of Cd^{2+} , the color changes from yellowish green to light brown, whereas no change in color of **1** is observed on addition of Mn^{2+} . The color changes are illustrated in Fig. 5. That an additional pyridine ring does help metal ion binding is evident from the fact that our previously reported DPP derivative^{16–18} bearing a cyano functionality does not show a noticeable change in the absorption spectrum on addition of Mn^{2+} , Co^{2+} , Ni^{2+} , Zn^{2+} and Cd^{2+} ions. With Cu^{2+} , a decrease in absorbance of the 421 nm band is observed. This corresponds to a K value of $2.27 \times 10^4 \text{ M}^{-1}$, which is two orders of magnitude less than that observed for the present system.

Anion sensing

Fig. 6 shows the change in absorption spectra of **1** on addition of F^- in CH_3CN solution. Upon addition of tetrabutylammonium fluoride (TBAF), the peak around 420 nm disappears, while a new band at 490 nm appears with an isosbestic point at 458 nm indicating equilibrium between **1** and **1**· F^- during the course of titration. The binding is associated with a color change from yellowish green to red and is observable by the naked eye. With other halogen anions and ClO_4^- , no color change was observed. This observation can be attributed to the small size of the F^- compared to the other anions. The binding constant for F^- complexation is estimated as $4.9 \times 10^3 \text{ M}^{-1}$. Restoration of the original spectrum of the sensor system from this sensor- F^- adduct upon addition of a trace amount of water/methanol not only suggests that the complexation between F^- and **1** is reversible in nature but also lends further support to the proposition that hydrogen-bonding is involved in the binding between the sensor and F^- .

Comparison of the binding constant values reveals that **1** binds the cations much more strongly (K values are two orders of magnitude higher) compared to the F^- . The X-ray structure of

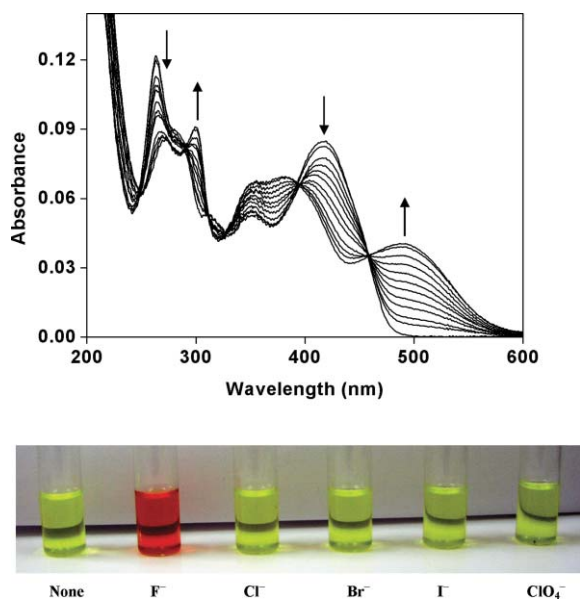


Fig. 6 Top: Absorption spectral changes observed for **1**, upon addition of F^- ion in CH_3CN at 298 K. $[1] = 6.5 \times 10^{-6}$ M; $[F^-] = (0, 2.33, 3.98, 6.29, 8.92, 12.18, 16.39, 21.21, 32.88, 42.14, 54.22, 68.9) \times 10^{-5}$ M. Bottom: Color changes observed for **1** in CH_3CN upon the addition of anions (as TBA⁺ salts). From left to right: none, F^- , Cl^- , Br^- , I^- and ClO_4^- .

4 clearly reveals that the pyridine nitrogen atom is involved in binding of the metal ions. It is already well known that hydrogen bonding interaction between F^- and pyrrole NH moieties is responsible for binding of F^- .⁹⁻¹⁸ Binding between the DPP moiety and F^- was explained with the help of a model,⁹ supported by theoretical calculations in our previously reported work.¹⁸ According to this model, the binding of F^- is facilitated by rotation of the pyrrole rings of DPP moieties in such a way that the NH protons are directed towards the lone pairs of the anion.^{9,18} A rotation to a different plane of such type is expected to allow the pyrrole rings to assume 'bite angle' suitable for the size of F^- and to position them away from the pyrazine chromophore, leading to perturbation in the orbital overlap between the pyrrole and pyrazine subunits.

Although, generation of a new peak around 500 nm is common to both cation and F^- titrations, careful examination of Fig. 5 and 6 reveals that the spectra for the finally formed $1 \cdot M^{2+}$ ($M = Co, Ni, Cu, Zn$) and $1 \cdot F^-$ complexes are different. The appearance of a long wavelength band on absorption titration can perhaps be attributed to an enhanced conjugation between the pyrrole and pyridopyrazine rings on complexation. The X-ray crystallographic studies suggest that the dihedral angles between the pyrrole and pyridopyrazine rings are reduced to some extent on metal complexation allowing a better conjugation. The color change for F^- binding can be explained with the help of a model which has been used to explain similar observation for other DPP compounds previously.^{9,18}

Sensing in the presence of competing ions

Since the present system consists of two distinct binding sites for the metal ions and F^- , we thought it appropriate to examine the effect of competing F^- ion on the binding ability of **1** for metal ions and *vice versa*. These experiments have been carried out in two

different manners. First, we have titrated **1** with F^- (using TBAF) in the presence of 2 equivalents of metal ions, M^{2+} . Second, we have titrated **1** with M^{2+} in the presence of 100 equivalents of TBAF. We chose Zn^{2+} and F^- for the dual sensing experiment as the Zn^{2+} salts are colourless and it is possible to observe distinct changes due to metal complexation/decomplexation without any interference from the colour of the salts. The spectral changes are shown in Fig. 7. As can be seen, initial titration of **1** and two equivalents of Zn^{2+} with TBAF results in a drastic reduction of the intensity of the 500 nm band suggesting sequestering of the metal ion to form an ion pair with F^- ion in solution, as has been recently observed in some cases.^{29,30} However, as expected, when sequestering of the metal ion is complete, further addition of F^- ion leads to expected enhancement of the intensity of the 500 nm band due to complexation of F^- ion. The binding constant of **1** with F^- in the presence of 2 equivalents of Zn^{2+} is estimated as $550 M^{-1}$, which is almost one order of magnitude less than that observed in the absence of competing metal ions. In the second experiment, which is carried out in the presence of 100 equivalents of F^- , addition of Zn^{2+} ion leads to a gradual reduction of the intensity of the 500 nm band due to the sequestering of F^- ion. The fact that the concentration of F^- ion in solution is far in excess of the Zn^{2+} ion, the condition in which all the F^- is completely uncomplexed is never met in this case and hence, enhancement of the 500 nm band intensity at a later stage, as has been noticed in the previous experiment, is not observed in this case. Moreover, the presence of large concentration of F^- in the solution engages the metal ions in ion pair formation in solution rather than engaging them in complexation. We repeated similar experiments with other metal ions such as Ni^{2+} and Cu^{2+} that do not have such high affinity towards F^- . With these metal ions, the sharp drop of absorption

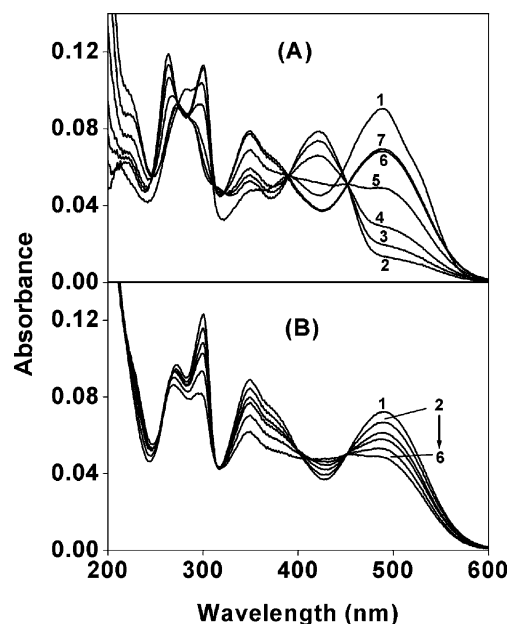


Fig. 7 Change in absorption spectra of (A) **1** ($6.5 \mu M$) on addition of Zn^{2+} ($[Zn^{2+}] = 13 \mu M$, spectrum 1) and then, titration with TBAF, $[F^-] = (2.03, 10.12, 20.18, 40.11, 79.21, 154.51) \times 10^{-5}$ M (spectra 2–7); (B) **1** ($6.5 \mu M$) on addition of TBAF ($[F^-] = 6.5 \times 10^{-4}$ M, spectrum 1) and then, titration with Zn^{2+} , $[Zn^{2+}] = (0.45, 0.85, 1.16, 1.78, 2.96) \times 10^{-3}$ M (spectra 2–6).

shown in Fig. 7(A) could not be observed because of high binding constant of **1** with the metal ions and low affinity of these metal ions with F⁻. Nevertheless, it is evident that although **1** contains distinct binding sites for both anion and cation, simultaneous binding of both the species, as observed exploiting the allosteric effect,³¹ through-bond electrostatic effect³² or to the host as an associated ion-pair,²⁹ is not possible in this case unless the total concentration of the two species is much less than what a particular binding site can accommodate.

Summary

In summary, the DPP derivative **1** has been synthesized and characterized by different methods. The crystal structures of **1** and **4**, which are essential for an understanding of the change in orientation of pyrrole rings on metal complexation and determining the coordinating site of the metal, have been determined. The binding constants of **1** with several transition metal ions have been found to be two orders of magnitude higher than that for the F⁻ in acetonitrile. The sensing of the metal ions and F⁻ is visible by naked eye observation of the colour change of the system. We are currently exploring the signaling behaviour of more such dipyrrolyl derivatives endowed with suitable cation binding substituents.

Acknowledgements

T. G. and A. S. thank the Council of Scientific and Industrial Research, New Delhi and Department of Science and Technology, New Delhi for financial support of this work. The UPE program of the University Grants Commission, New Delhi is gratefully acknowledged for some of the instrumentation facilities.

References

- (a) *Supramolecular Chemistry*, ed. J. M. Lehn, VCH, Weinheim, 1995; (b) V. Balzani, A. Juszis, A. M. Venturi, S. Campagna and S. Serroni, *Chem. Rev.*, 1996, **96**, 759; (c) A. P. de Silva, H. Q. N. Gunaratne, T. Gunnlaugsson, A. J. M. Huxley, C. P. McCoy, J. T. Rademacher and T. E. Rice, *Chem. Rev.*, 1997, **97**, 1515; (d) Luigi Fabrizzi, Special Issue on Luminescent Sensors, *Coord. Chem. Rev.*, 2000, **205**, (editor).
- (a) *Supramolecular Chemistry of Anions*, ed. A. Bianchi, K. Bowman-James and E. Garcia-Espana, Wiley-VCH, New York, 1997; (b) P. D. Beer and P. A. Gale, *Angew. Chem., Int. Ed.*, 2001, **40**, 486; (c) Philip A. Gale, Special Issue on Synthetic Anion Receptor Chemistry, *Coord. Chem. Rev.*, 2003, **240**, (editor).
- (a) U. E. Spichiger-Keller, *Chemical Sensors and Biosensors for Medical and Biological Applications*, Wiley-VCH, Berlin, 1998; (b) O. S. Wolfbeis, in *Biomedical Optical Instrumentation and Laser-Assisted Biotechnology*, ed. A. M. Verga Scheggi, Kluwer, Dordrecht, 1996.
- (a) P. A. Gale, *Coord. Chem. Rev.*, 2003, **240**, 191; (b) J. M. Mahoney, K. A. Stucker, H. Jiang, I. Carmichael, N. R. Brinkmann, A. M. Beatty, B. C. Noll and B. D. Smith, *J. Am. Chem. Soc.*, 2005, **127**, 2922; (c) D. R. Turner, E. C. Spencer, J. A. K. Howard, D. A. Tocher and J. W. Steed, *Chem. Commun.*, 2004, 1352; (d) S. L. Tobey and E. V. Anslyn, *J. Am. Chem. Soc.*, 2003, **125**, 14807.
- (a) P. G. Plioger, P. A. Tasker and S. G. Galbraith, *Dalton Trans.*, 2004, 313; (b) C. B. Smith, A. K. W. Stephens, K. S. Wallwork, S. F. Lincoln, M. R. Taylor and K. P. Wainwright, *Inorg. Chem.*, 2002, **41**, 1093; (c) L.-L. Zhou, H. Sun, H.-P. Li, H. Wang, X.-H. Zhang, S.-K. Wu and S.-T. Lee, *Org. Lett.*, 2004, **6**, 1071.
- (a) G. G. Talanova, H.-S. Hwang, V. S. Talanov and R. A. Bartsch, *Anal. Chem.*, 2001, **73**, 5260; (b) J. V. Ros-Lis, R. Martinez-Manez, K. Rurack, F. Sancenon, J. Soto and M. Spieles, *Inorg. Chem.*, 2004, **43**, 5183; (c) E. Arunkumar, A. Ajayaghosh and J. Daub, *J. Am. Chem. Soc.*, 2005, **127**, 3156; (d) T. Gunnlaugsson, J. P. Leonard and N. S. Murray, *Org. Lett.*, 2004, **6**, 1557; (e) L. Jia, Y. Zhang, X. Guo and X. Qian, *Tetrahedron Lett.*, 2004, **45**, 3969.
- (a) K. L. Kirk, *Biochemistry of the Halogens and Inorganic Halides*, Plenum Press, New York, 1991, p. 58; (b) A. Wiseman, *Handbook of Experimental Pharmacology XX/2, Part 2*, Springer-Verlag, Berlin, 1970, pp. 48–97.
- (a) K. A. Nielsen, J. O. Jeppesen, E. Levillain and J. Becher, *Angew. Chem., Int. Ed.*, 2003, **42**, 187; (b) H. Miyaji, W. Sato and J. L. Sessler, *Angew. Chem., Int. Ed.*, 2000, **39**, 1777.
- C. B. Black, B. Andrioletti, A. C. Try, C. Ruiperez and J. L. Sessler, *J. Am. Chem. Soc.*, 1999, **121**, 10438.
- P. Anzenbacher, Jr., A. C. Try, H. Miyaji, K. Jursikova, V. M. Lynch, M. Marquez and J. L. Sessler, *J. Am. Chem. Soc.*, 2000, **122**, 10268.
- T. Mizuno, W.-H. Wei, L. R. Eller and J. L. Sessler, *J. Am. Chem. Soc.*, 2002, **124**, 1134.
- P. Anzenbacher, Jr., D. S. Tyson, K. Jursikova and F. N. Castellano, *J. Am. Chem. Soc.*, 2002, **124**, 6232.
- J. L. Sessler, H. Maeda, T. Mizuno, V. M. Lynch and H. Furuta, *Chem. Commun.*, 2002, 862.
- J. L. Sessler, H. Maeda, T. Mizuno, V. M. Lynch and H. Furuta, *J. Am. Chem. Soc.*, 2002, **124**, 13474.
- D. Aldakov and P. Anzenbacher, Jr., *Chem. Commun.*, 2003, 1394.
- J. L. Sessler, G. D. Pantos, E. Katayev and V. M. Lynch, *Org. Lett.*, 2003, **5**, 4141.
- T. Ghosh and B. G. Maiya, *Proc. Indian Acad. Sci. (Chem. Sci.)*, 2004, **116**, 17.
- T. Ghosh, B. G. Maiya and M. W. Wong, *J. Phys. Chem. A*, 2004, **108**, 11249.
- D. Behr, S. Brandange and B. Lindstrom, *Acta Chem. Scand.*, 1973, **27**, 2411.
- M. C. Venuti, *Synthesis*, 1982, 61.
- D. D. Perrin, W. L. F. Armarego and D. R. Perrin, *Purification of Laboratory Chemicals*, Pergamon Press, New York, 1980.
- (a) *SMART version 5.630 and SAINT-plus version 6.45*, Bruker-Nonius Analytical X-ray Systems Inc., Madison, WI, USA, 2003; (b) G. M. Sheldrick, *SADABS Empirical Absorption Correction Program*, University of Göttingen, Göttingen, Germany, 1997; (c) G. M. Sheldrick, *SHELXTL: Structure Determination Programs, Versions 5.1*; Bruker-Nonius Analytical X-ray Systems Inc., Madison, WI, USA; (d) A. L. Spek, *PLATON A Multipurpose Crystallographic Tool*, Utrecht University, Utrecht, The Netherlands, 2002.
- I. B. Berlman, *Handbook of Fluorescence Spectra of Aromatic Molecules*, Academic Press, New York, 2nd edn, 1971, p. 322.
- S. Banthia and A. Samanta, *J. Phys. Chem. B*, 2002, **106**, 5572.
- A. K. Connors, *Binding Constants: The Measurement of Molecular Complex Stability*, Wiley-VCH, New York, 1987.
- A. P. de Silva, I. M. Dixon, H. Q. N. Gunaratne, T. Gunnlaugsson, P. R. S. Maxwell and T. E. Rice, *J. Am. Chem. Soc.*, 1999, **121**, 1393.
- J. L. Manson, *Inorg. Chem.*, 2003, **42**, 2602.
- N. J. Turro, *Modern Molecular Photochemistry*, Benjamin/Cummings Publishing, Menlo Park, CA, 1978, p. 108.
- R. Shukla, T. Kida and B. D. Smith, *Org. Lett.*, 2000, **2**, 3099.
- G. Tumcharern, T. Tuntulani, S. J. Coles, M. B. Hursthouse and J. D. Kilburn, *Org. Lett.*, 2003, **5**, 4971.
- (a) S. Kubik and R. Goddard, *J. Org. Chem.*, 1999, **64**, 9475; (b) P. D. Beer, P. K. Hopkins and J. D. McKinney, *Chem. Commun.*, 1999, 1253.
- (a) P. D. Beer and J. B. Cooper, *Chem. Commun.*, 1998, 129; (b) T. Tozawa, Y. Misawa, S. Tokita and Y. Kubo, *Tetrahedron Lett.*, 2000, **41**, 5219.